lymphatics

MDPI

Review

Advances and Techniques in Medical Imaging and Minimally Invasive Interventions for Disorders of the Central Conducting and Mesenteric Lymphatic System

Frederic J. Bertino [1,*] and Kin Fen Kevin Fung [2]

[1] Department of Radiology, Interventional Radiology Section, NYU Grossman School of Medicine, NYU Langone Health, New York, NY 10017, USA
[2] Department of Radiology, Hong Kong Children's Hospital, Hong Kong, China; gwevin@gmail.com
* Correspondence: fredbertino.ir@gmail.com

Abstract: The central conducting lymphatics (CCL) and mesenteric lymphatic systems are responsible for lipid absorption, fluid regulation, and protein delivery into the bloodstream. Disruptions in these systems can result in debilitating conditions such as chylothorax, plastic bronchitis, post-operative lymphocele, protein-losing enteropathy (PLE), and chylous ascites. Advances in imaging techniques, including magnetic resonance lymphangiography (MRL), computed tomography lymphangiography (CTL), and fluoroscopic lymphangiography, allow for detailed anatomic and functional evaluation of the lymphatic system, facilitating accurate diagnosis and intervention by interventional radiologists. This review explores the embryology, anatomy, and pathophysiology of the lymphatic system and discusses imaging modalities and interventional techniques employed to manage disorders of the conducting lymphatics in the chest and abdomen. Thoracic duct embolization (TDE), percutaneous transhepatic lymphatic embolization (PTLE), and sclerotherapy are highlighted as effective, minimally invasive approaches to treat lymphatic leaks and obstructions and have shown high success rates in reducing symptoms and improving patient outcomes, particularly when medical management fails. This review seeks to demonstrate how anatomical imaging can facilitate minimally invasive procedures to rectify disorders of lymphatic flow.

Keywords: central conducting lymphatics; lymphangiography; magnetic resonance lymphangiography; thoracic duct embolization; protein-losing enteropathy; chylothorax; lymphocele; essential embryology and anatomy of the lymphatic system

check for updates

Academic Editor: Toshio Ohhashi

Received: 19 December 2024
Revised: 29 January 2025
Accepted: 20 February 2025
Published: 19 March 2025

Citation: Bertino, F.J.; Fung, K.F.K. Advances and Techniques in Medical Imaging and Minimally Invasive Interventions for Disorders of the Central Conducting and Mesenteric Lymphatic System. *Lymphatics* **2025**, *3*, 8. https://doi.org/10.3390/lymphatics3010008

Copyright: © 2025 by the authors. Licensee MDPI, Basel, Switzerland. This article is an open access article distributed under the terms and conditions of the Creative Commons Attribution (CC BY) license (https://creativecommons.org/licenses/by/4.0/).

1. Background and Introduction

The central conducting lymphatics (CLL) are responsible for the maintenance of fluid homeostasis, absorption of long-chain lipids from the small bowel, delivery of protein synthesized in the liver into the bloodstream, and immune regulation [1]. The CCL are composed of three interconnecting lymphatic networks, which are responsible for the drainage of hepatic, mesenteric, and soft tissue lymph [1]. These systems connect to the cisterna chyli and thoracic duct, which ultimately drains into the venous circulation. The hepatic lymph constitutes about 40% of the total lymphatic flow and is protein-rich and fat-free [1,2].

The liver's lymphatic system in healthy individuals comprises vessels in the portal region, hepatic venous area, and sub-capsular zone [3]. The portal tract lymphatic vessels are the main drainage site, producing about 80% of the liver's lymph. These capillaries

merge into larger vessels wrapped by lymphatic muscle cells outside the liver, which facilitate lymph flow to hepatic or hilar nodes in the liver's hilum. From there, lymph travels to celiac lymph nodes and then to the cisterna chyli at the thoracic duct's lower extremity [2].

Compared to the embryogenesis of other arteries and veins, the lymphatic system arises substantially later, thought to originate at week 6–7 of gestation, approximately 1 month after the first blood vessels [4,5]. The first structures to arise are jugular lymphatic sacs, adjacent to the jugular section of the cardinal vein. The formation of lymphatic channels is thought to occur in a centrifugal model, suggesting that primary lymph sacs arise from endothelial cell origins from embryonic veins, followed by the subsequent endothelial growth of the lymph sacs into surrounding tissues. While the centripetal (origins of lymphatics beginning in peripheral tissues and growing centrally) may occur in nature, the centrifugal model of lymphogenesis is more regarded to occur in higher mammals [6].

Lymphogenesis is thought to occur in four distinct stages, including lymphatic competence, commitment, specification, and coalescence/maturation. Lymphatic competence is defined as the cellular capacity to respond to cell signaling to initiate lymphatic differentiation, and the signals responsible for lymphatic development are unique to lymphogenesis and distinct from blood vessel development [7–9]. Lymphatic commitment is characterized by the cellular expression of Prox1, a nuclear transcription factor unique to lymphatic cell lineage, which commits venous endothelium to lymphatic function [10]. Specification involves the expression of distinguished molecular markers unique to lymphatic cells including podoplanin, VEGFR3, and neuropilin-2 [11–13]. Finally, vascular coalescence and maturation occur as lymphatic channels develop into conducting, valved, and collecting vessels.

Mature coalesced, and conducting lymphatics operate with fluid extravasation at the capillary level in mature tissue, where fluid uptake occurs via blind-ending pouches of valveless single-endothelial cells [14]. Primary lymphatics have valves and shuttle fluid to contractile muscular units of lymphatics called lymphangions [15]. Lymphatic flow occurs from peripheral to central, and superficial to deep. Lymph-collecting vessels are characterized as either superficial or deep, depending on their relationship to deep fascia. The lymph node is a merger point for collecting lymphatics [16,17].

The left upper extremity and lower extremities are drained via the thoracic duct. In the abdomen, coalescent channels of systemic and mesenteric lymphatics join the thoracic duct at the cisterna chyli. The right upper extremity is drained to the right lymphovenous angle at the confluence of the right internal jugular and subclavian veins (Figure 1). While this anatomic configuration/macrostructure is considered conventional, it accounts for approximately 40–60% of the population [18]. There are six well-described anatomic variants of the macrostructure of the lymphatic system, including patients without an identifiable cisterna chyli (>30%), a left-sided posterior aortic thoracic duct (36%), a right thoracic duct (6%), a duplicated thoracic duct, or a thoracic duct with multiple terminations, plexiform lymphatic channels without a solitary thoracic duct, and multiple termini of the thoracic duct into the venous angle, subclavian vein, or internal jugular vein [19]. Interventional radiologists take advantage of lymph nodes (for example, inguinal) with needle access that facilitates the injection of contrast agents for lymphatic visualization and intervention.

Lymphatic capillaries near the hepatic vein join into 5–6 large vessels that, along with the inferior vena cava, pass through the diaphragm to posterior mediastinal lymph nodes. The sub-capsular lymphatic vessels on the liver's convex surface lead to regional nodes like the diaphragmatic lymph nodes in the thoracic region, eventually flowing to mediastinal nodes, following a similar route as the hepatic vein-associated lymphatics [2,3].

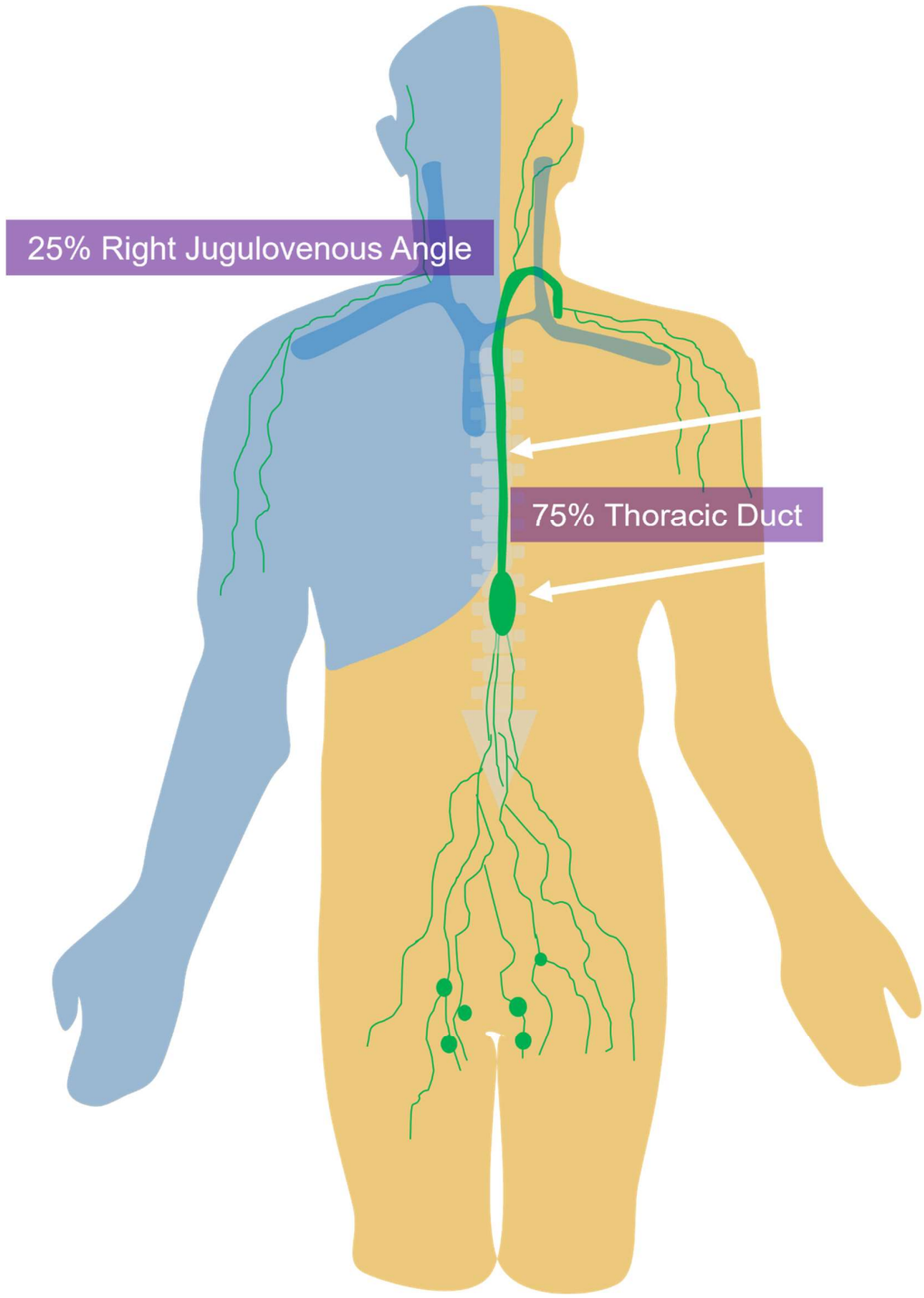


Figure 1. Conventional anatomy of the central conducting lymphatics and usual drainage pathways from the extremities and trunk.

2. Imaging of the Central Conducting Lymphatics

In current medical practice, the central conducting lymphatic system may be imaged using many imaging modalities and techniques. These techniques include magnetic resonance lymphangiography (MRL), computed tomography lymphangiography (CTL), fluoroscopic lymphangiography, and lymphoscintigraphy. Techniques involving diagnostic and therapeutic modalities (MRL, CTL, and fluoroscopic) will be discussed in this review. Indications for lymphatic imaging include chylothorax, chylous ascites, lymphedema,

protein-losing enteropathy, and lymphorrhea of any kind, as well as for anatomic survey of the lymphatics, such as in the case of central conducting lymphatic anomaly.

3. Magnetic Resonance Lymphangiography

MRI Lymphangiography (MRL) offers higher spatial and temporal resolution compared to lymphoscintigraphy and can provide both functional and anatomical information in a single imaging examination [20,21]. The temporal resolution allows for the visualization of lymphatic flow in real-time and is considered the standard of care when evaluating patients for lymphatic intervention or diagnosing lymphatic leaks. However, the examination requires multiple acquisitions to monitor lymphatic flow over time and can be lengthy in duration, with some pediatric patients requiring sedation or anesthesia for the examination. Venous contamination of intra-nodal gadolinium contrast agents can lead to some misinterpretation [20,21].

General Technique

MRI zone III is the portion of the MR suite just adjacent to the room that holds the MR scanner. Patients in this zone are screened for metallic objects and positioned on a mobile detachable MR-compatible table in supine position. If patients require anesthesia or sedation, it is administered at this time. Under ultrasound guidance, needle access is obtained with 22- or 25-gauge needles into lymph nodes, with 1–2 lymph nodes targeted on either side of the body [22]. Care is taken to position the needle tip at the transitional zone between the cortex and hilum of the lymph node to best avoid extravasation of contrast [23]. When imaging the mesenteric or thoracic lymphatics, the lymph node of choice is often the inguinal chain as these are superficial and regularly seen in most patients. A small volume of saline or contrast-enhanced US agent is injected into the lymph node to confirm access and to confirm that no extravasation has occurred [24,25]. The access needles are then secured into place with tissue adhesive. Long plastic intravenous connector tubing is flushed with gadolinium-containing MR contrast media and attached to the needles. Dose considerations in pediatric patients are recommended at 0.1 mmol/kg in a 1:2 or 1:3 dilution with the normal saline split between the two syringes. Adult patients may tolerate 5–10 cc gadolinium-based contrast per lymph node.

Conventional needle access in the groin or mesenteric lymph nodes does not opacify the liver lymphatics. In order to image the hepatic lymphatic flow, it is essential to obtain needle access in the peripherally located intrahepatic lymphatic channels, which is the technically most challenging step of the procedure. Under ultrasound guidance, a 25G spinal needle is placed in the peri-portal echogenic area (Figure 2A). The needle position is then confirmed with an injection of 0.5–1 mL of water-soluble iodinated contrast under fluoroscopic screening [26,27]. It is important to recognize the spidery appearance of hepatic lymphatic channels (Figure 2B) in contradistinction to the more tubular-looking intrahepatic ducts (Figure 2C) Opacification of fast flow tubular structures usually indicate cannulation of hepatic veins and portal veins and require needle repositioning.

In institutions with hybrid MR-Angiography suite, after intranodal and/or intrahepatic needle access is secured, the patient is transferred to the same tabletop for MR scanning, minimizing the risk of needle dislodgement [28]. In institutions where the angiography machine and MR scanner are in different rooms, it is beneficial to move the patient from the angiography table to a detachable MR table for transferal to the MR scanner in Zone 4. While needle dislodgement is still possible during transfer between tabletops, this eliminates the need for further patient transfer in the MR scanner.

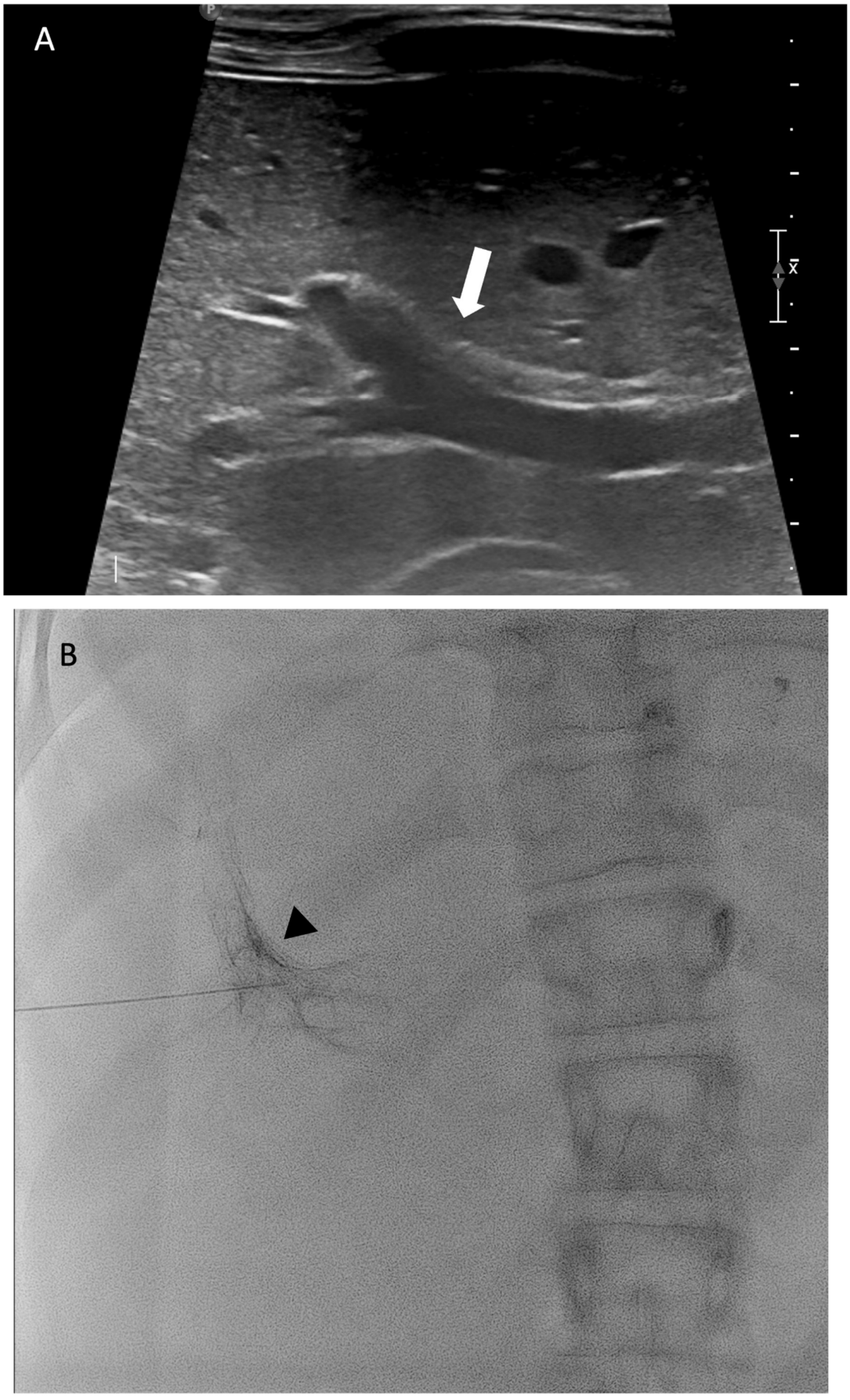


Figure 2. *Cont*.

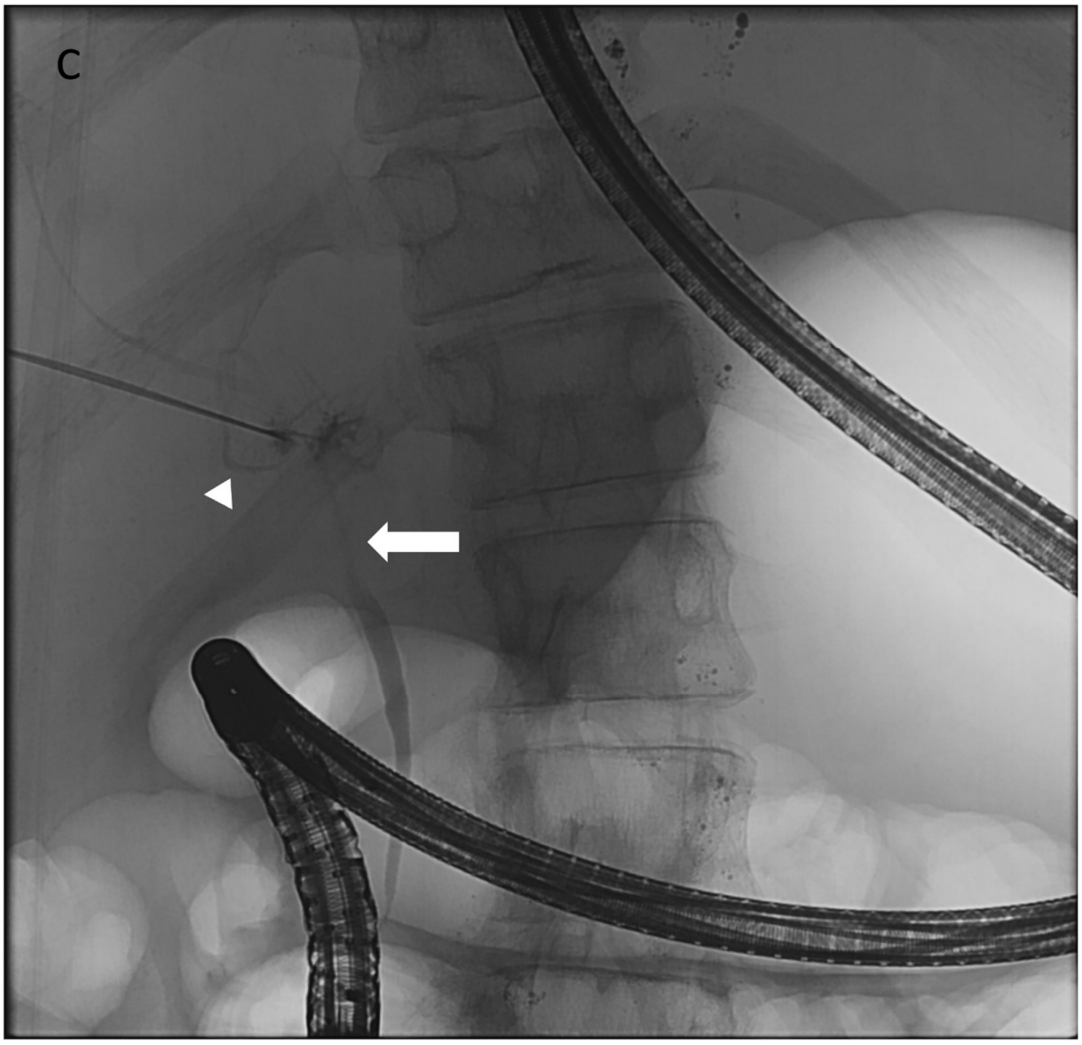


Figure 2. A 16-year-old girl with somatic KRAS mutation and protein-losing enteropathy. (**A**) Transverse US of liver demonstrated thickening of periportal echogenicity. White arrow indicates the target area of needle puncture for intrahepatic lymphangiogram. (**B**) Spot fluoroscopic image of liver showed typical appearance of intrahepatic periportal lymphatic channels as a fine reticular network (black arrowhead) surrounding portal vasculature. (**C**) Spot fluoroscopic image of liver showed lympho-biliary and lympho-venous communication upon contrast injection. A non-dilated biliary tree is opacified (white arrow). Curvilinear tubular channel with rapid washout indicates hepatic venous channels (white arrowhead).

When in zone IV, the table is connected to the MR scanner with special care not to disrupt needle positioning. The MR coil of choice is carefully positioned over the patient (Figure 3) and the scan begins. Two interventional radiology physicians remain in MR zone IV during the scanning process [22]. Depending on institutional protocols, a coronal T2-weighed sequence is acquired to obtain static information about the lymphatic system. This is then followed by the injection of a diluted gadolinium-based contrast agent (GBCA) at a dose of 0.1–0.2 mmol/kg, which is injected by hand at a rate of 0.5–1.0 mL/min. If multiple accesses are obtained in the liver and inguinal lymph nodes, the total dose of gadolinium will be equally divided between the number of access sites, and the intrahepatic lymphatics will be imaged first.



Figure 3. (**A**) Clinical photo shows position of intrahepatic (black arrow) and bilateral inguinal nodal needles (arrowheads). They were secured by clear adhesives to prevent dislodgement. (**B**) Clinical photo shows patient being transferred onto detachable MR table. Soft foam blocks were placed on the side of the MR table to elevate the torso coil to minimize movement of the intrahepatic needle.

After the pre-contrast enhanced images are complete, the manual injection of contrast at a very slow rate of injection begins. Protocols of imaging frequency differ between institutions but may include repeat imaging in intervals of 30 s–120 s, depending on the patient size. There are many protocols published describing the specific MRL protocol for nodal and intrahepatic MRL; however, generally accepted sequences include coronal T1-weighted images before contrast media injection, with post-contrast enhanced images obtained at set time intervals. For intrahepatic lymphangiograms, in healthy subjects, after initial opacification of periportal hepatic lymphatics, contrast should opacify peri-hilar lymphatics within 1 min. The cisterna chyli and thoracic duct should be visualized within 2–5 min. Pericholecystic enhancement is also considered a normal finding [29]. Occasionally subcapsular and hepatic venous lymphatics may also be seen. Termination of imaging may occur at the visualization of the venous angle or if chylous reflux is appreciated [22].

4. Computed Tomography Lymphangiography

Computed tomography lymphangiography (CTL) has the benefits of being significantly faster acquisitions of dynamic lymphatic flow compared to MRL and provides excellent spatial resolution. Anesthesia/sedation needs are less necessary in older patients given the significantly shorter procedure/imaging duration; however, the modality uses ionizing radiation to capture images which may be suboptimal in pediatric patients. Low-dose techniques are currently being developed, as in the case of using cone-beam CT for evaluating the systemic and hepatic lymphatics of smaller children [30].

Procedural techniques regarding needle access into the lymph nodes and intrahepatic are similar to those in MRL. Non-contrast imaging of the region of interest is then performed, and slow injection of ethiodized oil or water-soluble contrast is injected through the connector tubing into the lymph nodes with periodic imaging of the regions of interest to monitor dynamic contrast flow. Ethiodized oil provides better visualization of lymphatic channels but is contraindicated in patients with right-to-left shunts [31]. The CT is repeated within 60 min from the mid-neck to the inguinal access site. CTL can be therapeutic as well as diagnostic since ethiodized oil may act as an embolic agent and can be mixed with n-BCA glue to embolize visualized leaks [32]. Similarly, the thoracic duct may be targeted under CT guidance and provide options to perform thoracic duct disruption (TDD) or direct thoracic duct lymphangiography [32].

5. Fluoroscopic Lymphangiography

Fluoroscopic intra-nodal lymphangiography is a beneficial technique for the diagnosis of lymphatic disorders, leaks, and obstruction in real-time with live fluoroscopy. Cone-beam CT (CBCT) lymphangiography is an added technique capable of being performed on most angiography units and uses low-dose ionizing radiation to provide CT images for better characterization of lymphatic leaks and tissue resolution, particularly if water-soluble contrast is used [30]. Additional advantages of CBCT include the ability to assess the anatomy of the liver and central conducting lymphatics with multiplanar capabilities (Figures 4 and 5). When performed in an angiography suite, diagnosis and therapeutic intervention may be carried out in the same encounter. The technique can be performed for the imaging of the systemic and hepatic lymphatics [23,30].

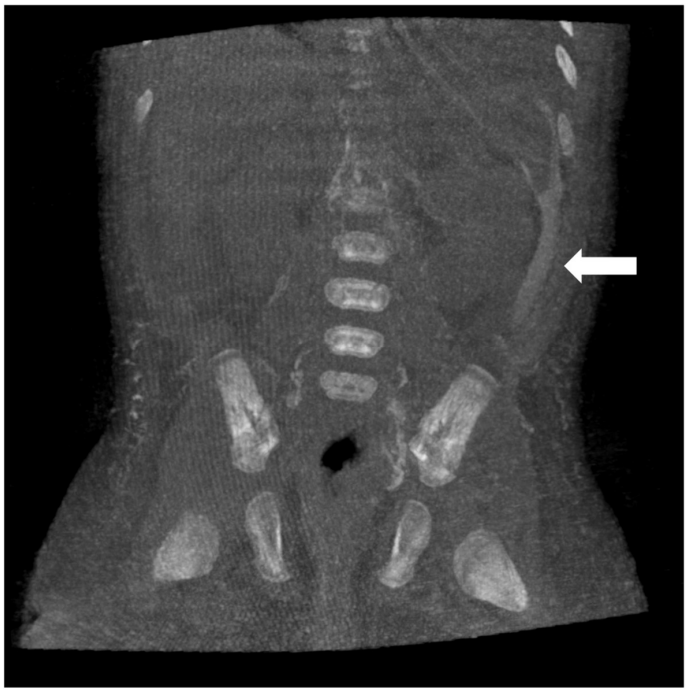
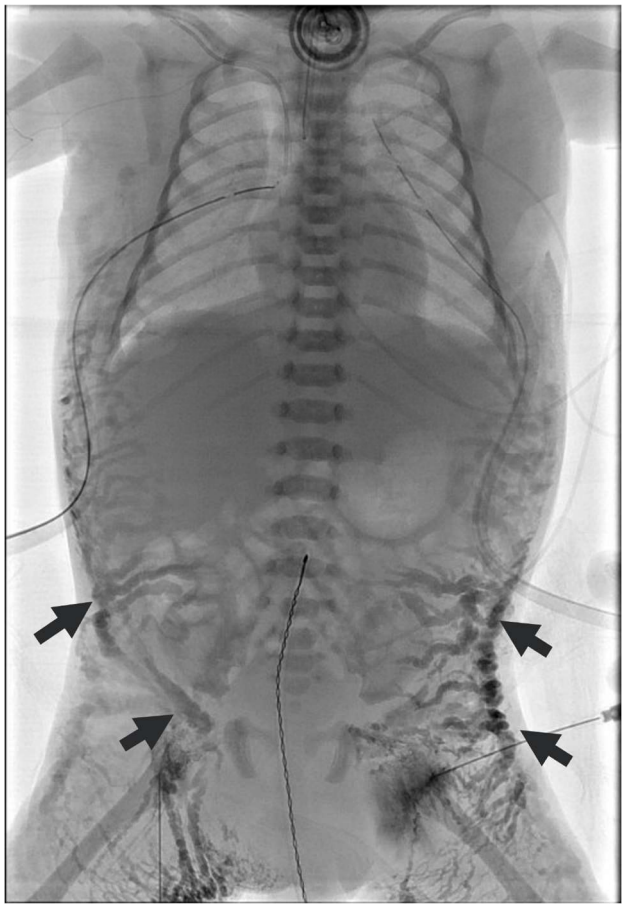
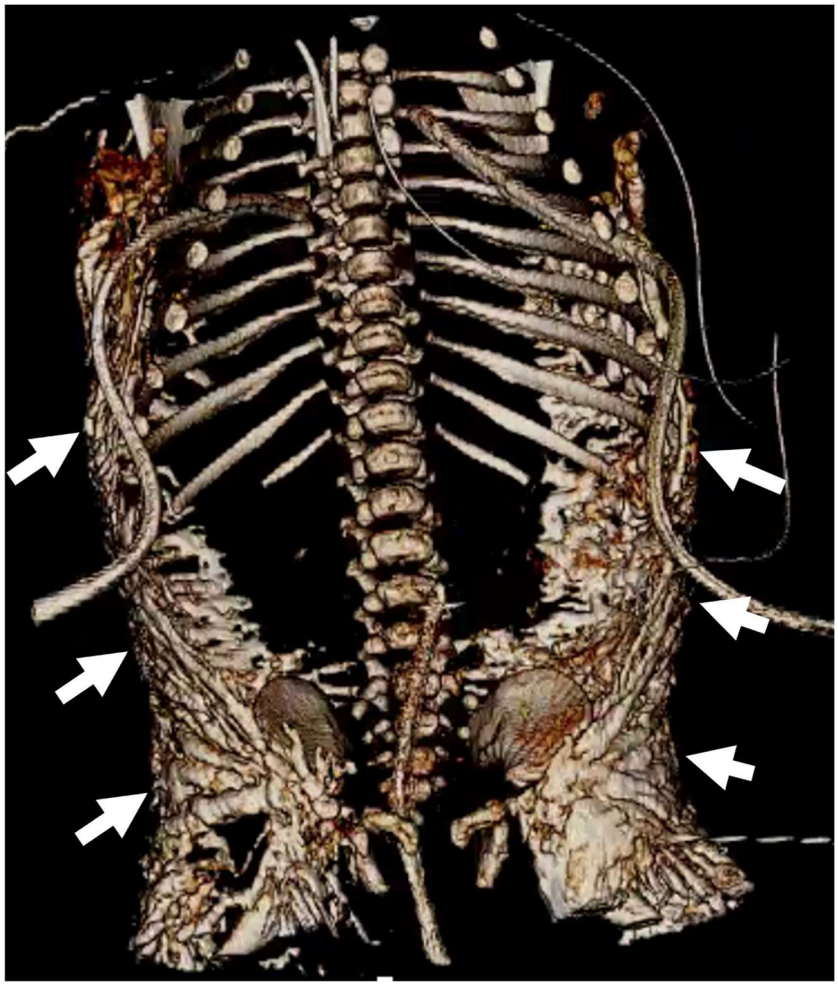


Figure 4. Coronal reformatted image of CBCT of a 56-day-old neonate with diffuse soft tissue edema. Contrast opacification of ascitic fluid (white arrow) confirmed the presence of chylous ascites. This finding was not seen on fluoroscopic images.



(**a**)

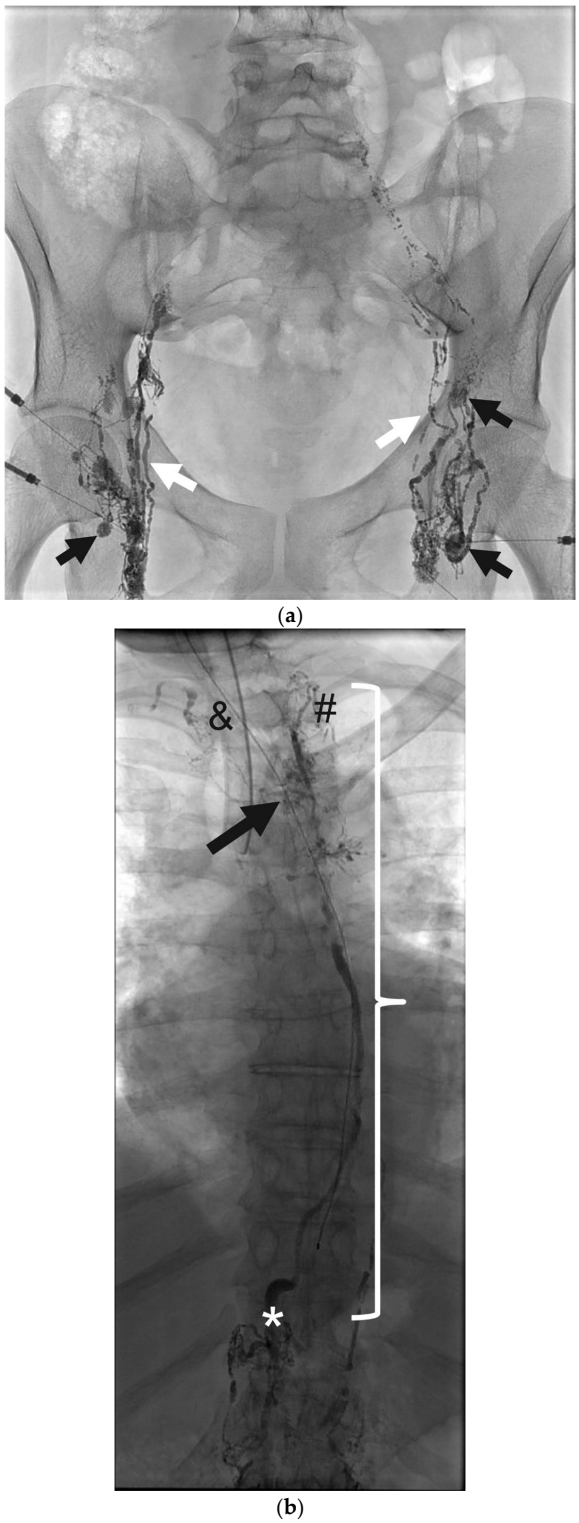
Figure 5. *Cont.*



(**b**)

Figure 5. (**a**) Antero-posterior fluoroscopic lymphangiogram of a 34-day-old neonate with congenital chylothorax. Black arrows demonstrate a preferential flow through the dermal lymphatics without filling of the central conducting lymphatics, which would be expected over the midline of the spine, consistent with a central conducting lymphatic anomaly (CCLA). (**b**) is a coronal 3D reformat from cone-beam CT images. The white arrows correspond to dermal lymphatics without lymphatic channels in the central midline.

Intranodal and intrahepatic needle access is performed in a similar fashion under ultrasound guidance as in MRL and CTL [23]. Ethiodized oil is injected at a rate of 0.2–0.4 mL/min, without exceeding 10–20 mL oil. Injection may be accomplished via an automatic or dedicated lymphangiogram pump, but manual injection may also suffice. Serial spot radiographs of the anatomic regions of interest are obtained every 5–10 min to monitor the progression of oil as it flows along the central conducting lymphatics. Anatomic landmarks include sentinel nodal groups in the expected chain downstream of the accessed node, cisterna chyli, and the thoracic duct (Figure 6). Reflux of contrast may also provide clinical clues [33] regarding downstream occlusion (duct disruption or ligation).



(**a**)

(**b**)

Figure 6. Conventional fluoroscopic lymphangiography technique and anatomy in a 54-year-old man with chylothorax after video-assisted thoracoscopic surgery. (**a**) Intranodal access is obtained with a 22- or 25-gauge needle into the inguinal lymph nodes under ultrasound guidance. Black arrows reflect lymph nodes opacified with ethiodized oil. The white arrows indicate long linear conducting lymphatic channels. (**b**) The thoracic duct. The cisterna chyli (*) opacifies first, with the long linear thoracic duct opacifying next, which drains the mesenteric lymphatics, and the lungs (bracket). The black arrow indicates the presence of a plexiform variant with some pulmonary lymphatic drainage at the level of the central airways. There is normal drainage into the left lymphovenous angle (#). However, an anatomical variant exists where the right upper extremity lymphatics drain into the thoracic duct and subsequently into the left lymphovenous angle (&), instead of directly into the right lymphovenous angle.

Fluoroscopic lymphangiography allows for direct access to the thoracic duct, performed under direct fluoroscopic-guided puncture with a long 22G needle via an anterior transabdominal route. Through this needle, a guidewire may be passed into the thoracic duct for dedicated thoracic duct imaging and intervention [23].

6. Chylothorax

Chylothorax is an accumulation of chyle between the lung and pleura, which most commonly results from trauma/injury to the thoracic duct. Idiopathic chylothorax can be seen in premature newborns, those with congenital heart disease, or RASopathy [34,35]. Esophagectomy is the most common cause of traumatic chylothorax, with incidence of 1.1–21% after surgery [36]. All iatrogenic causes of chylothorax are estimated at 54%, and video-assisted wedge resection of the lung is said to result in chylothorax occurring in 0.2% to 7% of the cases, depending on how involved the lung resection is [36]. Non-traumatic causes of chylothorax include malignancy, with the most common cause being lymphoma, followed by chronic lymphocytic leukemia, lung cancer, esophageal cancer, and metastasis; lymphatic disorders (lymphangiectasia syndromes, lymphangioleiomyomatosis, yellow nail syndrome, and Gorham's disease); infections (tuberculosis, histoplasmosis, and filariasis); congenital anomalies; and other medical conditions that affect venous and lymphatic pressures (cirrhosis, congestive heart failure, superior vena cava syndrome) [37,38].

The diagnosis of chylothorax occurs with a characteristic clinical history and elevated triglyceride levels over 110 mg/dL, along with reduced cholesterol levels (<200 mg/dL) in the pleural fluid [33]. Chylous effusions should similarly contain chylomicrons, as these fatty molecules are absorbed directly into the mesenteric lymphatics via lacteals without first-pass metabolism through the liver [39,40]. In patients who are malnourished, there is a small (1%) chance that a thoracic duct leak may be non-chylous (1%). Low triglyceride levels may also be seen in cases of cirrhosis or congestive heart failure, or if a transudative pleural effusion confounds the triglyceride level. In these cases, triglyceride electrophoresis on the fluid, total protein (elevated) and LDH (low), and cell count (>70% lymphocytes) can serve as diagnostic indicators of a pleural effusion made of lymphatic fluid [33,41].

The medical management of chylothorax in adult and pediatric patients after diagnosis is challenging, as there are no established guidelines, with trends varying between institutions [33]. The algorithm used in the authors' institution is detailed in Figure 7. Techniques for conservative management begin with a low-fat diet and transition away from an oral diet to total parenteral nutrition, the initiation of octreotide/somatostatin analog infusion to inhibit peristalsis of the contractile lymphangion and smooth muscle in central conducting lymphatics with the intention of diminishing flow through the central conducting lymphatics [42,43]; however, high-volume leaks are likely to fail when chest tube output is >500 cc/day for >2 weeks [42].

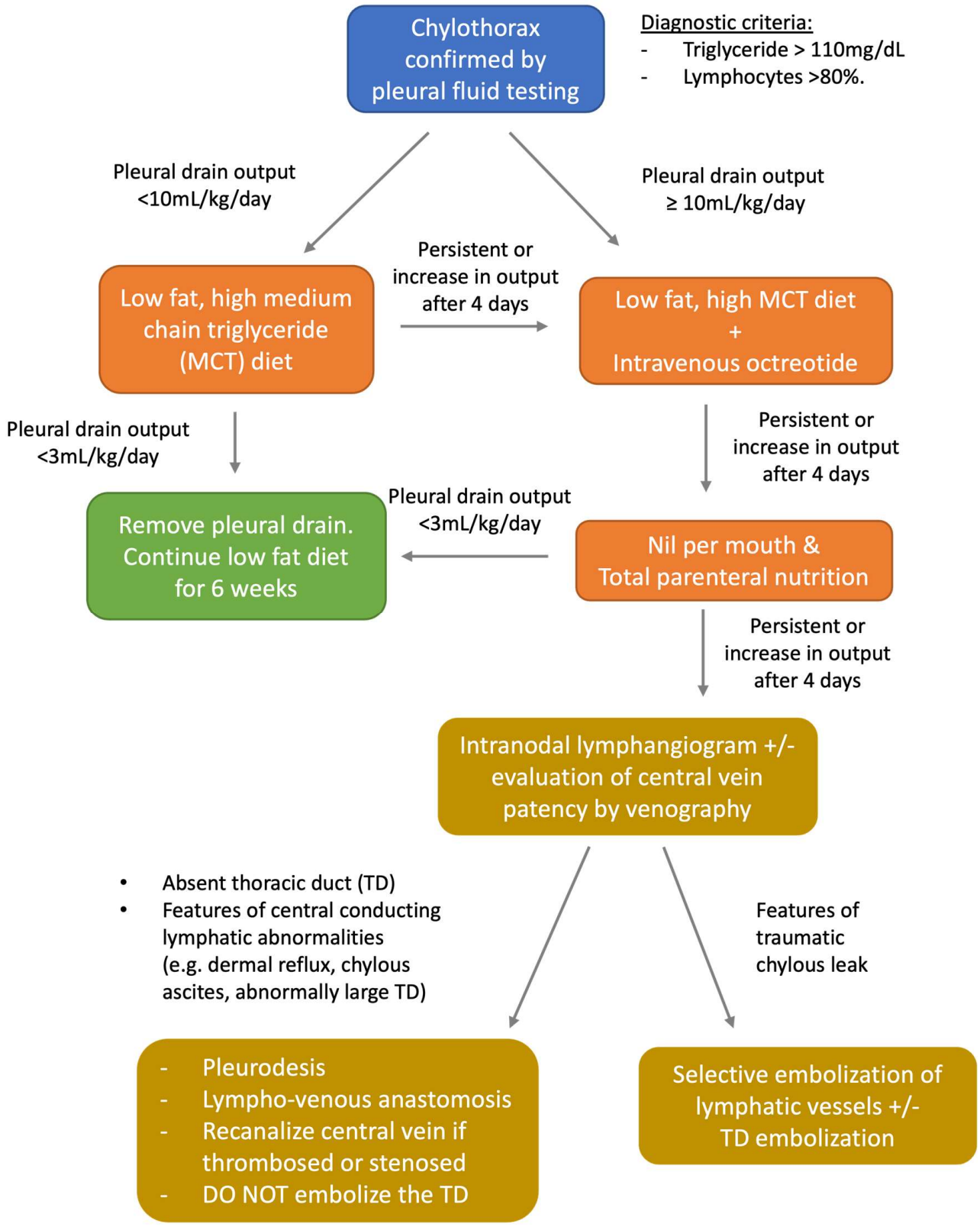


Figure 7. An algorithm detailing the imaging and treatment strategies of chylothorax.

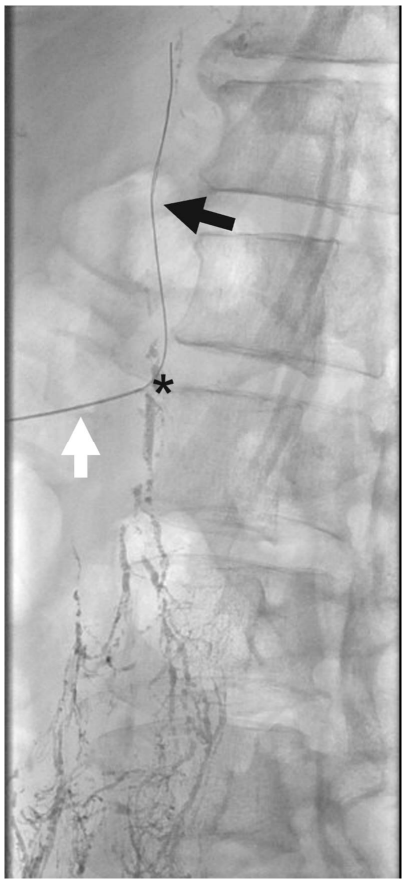
7. Plastic Bronchitis

Plastic bronchitis (PB) is a severe pulmonary condition characterized by the formation of thick casts in the airways from lymphatic exudate that take the appearance of branched airways and can lead to life-threatening airway obstruction [44,45]. Etiology

is multifactorial, with pediatric patients commonly affected by congenital heart disease (specifically after the Fontan procedure), asthma, and infectious/inflammatory processes. Adults may develop PB from similar causes, surgical procedures, abnormal lymphatic flow, or through unknown (idiopathic) causes. While the specific pathophysiology is still unknown, two types of PB casts have been described, with Type I casts associated with inflammatory diseases and Type II casts caused by mucofibrinous material in the airways forming plugs that obstruct the bronchopulmonary tree, without an inflammatory infiltrate [44–46]. Conservative management involves mucolytic medication, chest physiotherapy, and corticosteroids, with bronchodilators/saline having been shown to be ineffective [47]. There is possibly a role for mTOR inhibition (rapamycin) in decreasing chyle production [48], with thoracic duct embolization becoming the mainstay of treatment for this condition [49].

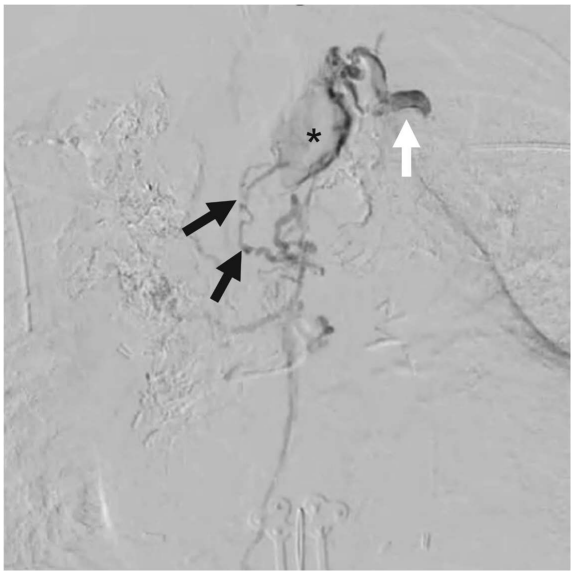
8. Thoracic Duct Embolization (TDE)

Fluoroscopic lymphangiography is carried out in the usual fashion described previously and the technique for cannulation of the thoracic duct has been described [50]. Access to the thoracic duct is performed with long 22- or 21-gauge needles with multiplanar imaging performed in real-time in an angiography suite. General anesthesia for the purposes of breath-holds during the procedure is important for needle-target accuracy. A technical description of the procedure for the management of chylothorax and plastic bronchitis is provided in Figures 8 and 9, respectively.

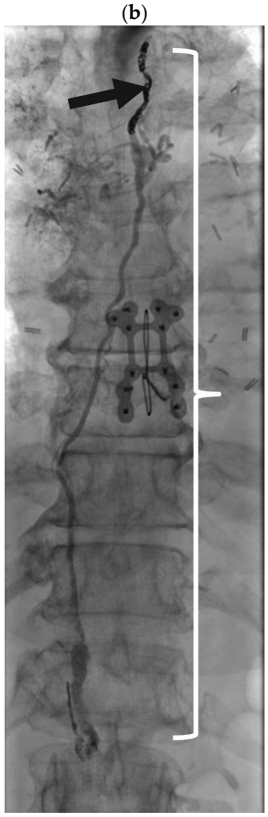


(**a**)

Figure 8. *Cont.*



(**b**)



(**c**)

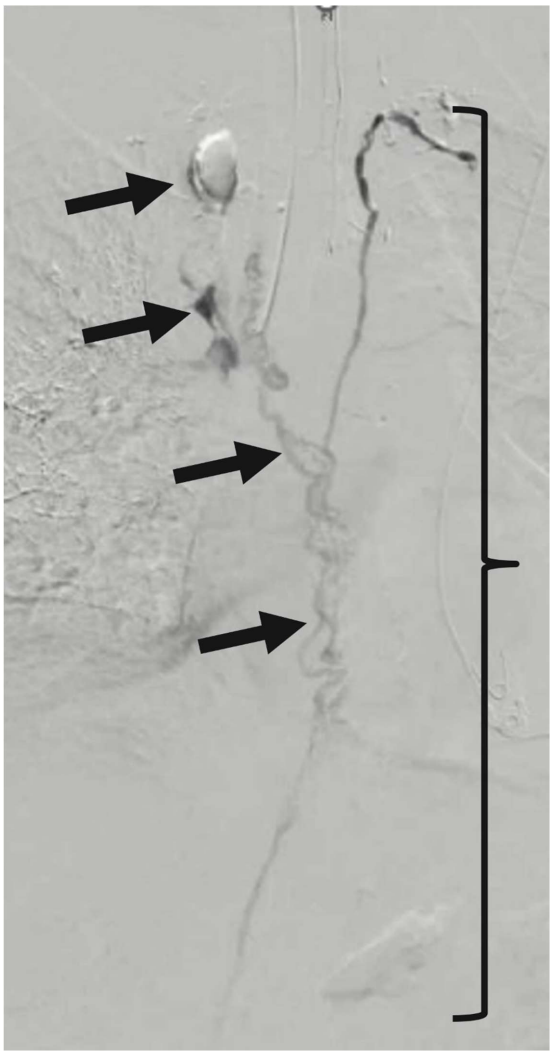
Figure 8. Thoracic duct embolization for chylothorax in a 54-year-old man after bilateral lung transplantation. (**a**) The white arrow indicates a 22G needle that has successfully punctured the cisterna chyli (*). The black arrow indicates a guidewire, inserted through the needle and used to catheterize the thoracic duct. The wire should track without resistance, indicating its location in a hollow tube. (**b**) Thoracic duct lymphangiogram. Water-soluble contrast is injected under digital subtracted angiography. The white arrow identifies the normal left-sided thoracic duct terminus. The black arrows show abnormal collateral drainage pathways to the right hemithorax, which are abnormal and contributory to chylothorax. A large leak (*) in the right chest is identified as the source of chylothorax. (**c**) The black arrow indicates the location of radio-opaque metallic coils used to embolize the thoracic duct terminus. This is performed to prevent liquid nBCA glue embolic from draining to the vein and embolizing to the lungs. The white bracket shows an opacified thoracic duct with glue, embolized in a 1:1 mixture of nBCA glue to ethiodized oil. The glue mixture is injected under real-time fluoroscopy and watched as the catheter is slowly retracted, and then promptly removed.

TDE has been shown to be a safe, efficacious, and durable procedure for the management of chylothorax and plastic bronchitis, with present-day success rates between 82% and 92% for spontaneous leaks and post-surgical leaks, respectfully [51]. The initial work by Cope et al. in 1999 first showed a 45% success rate in 11 patients that increased to >70% success rate in a cohort of 42 patients [52,53]. In 2010, Itkin et al. demonstrated a >90% technical success rate for TDE in 109 patients and a >70% success rate for thoracic duct disruption (fenestration of the duct and peri-ductal tissues to reduce central flow) [54]. A meta-analysis by Kim et al. in 2018 included 407 patients from 9 studies with >10 patients each and showed a >80% clinical success rate (cessation of chylothorax) after TDE, with >50% efficacy for ethiodized oil lymphangiography alone [55]. Finally, in works by Savla et al. and Majdalany et al., clinical success rates in children were reported at 64–94%, and those children without a central conducting flow disorder were reported to have cessation of chylothorax with a 100% clinical success rate when a leak could be identified and appropriately embolized [1,56,57]. Complications associated with lymphangiography and TDE are generally rare, but the overall complication rate has been reported at 14.3% and can include chronic leg swelling (8%), abdominal swelling (6%), and chronic diarrhea (12%), in the follow-up of a cohort of 78 patients [58]. In pediatric patients with congenital intracardiac shunts, the rare complication of paradoxical embolism and stroke from ethiodized oil has been reported [31].



(**a**)

Figure 9. *Cont.*



(**b**)

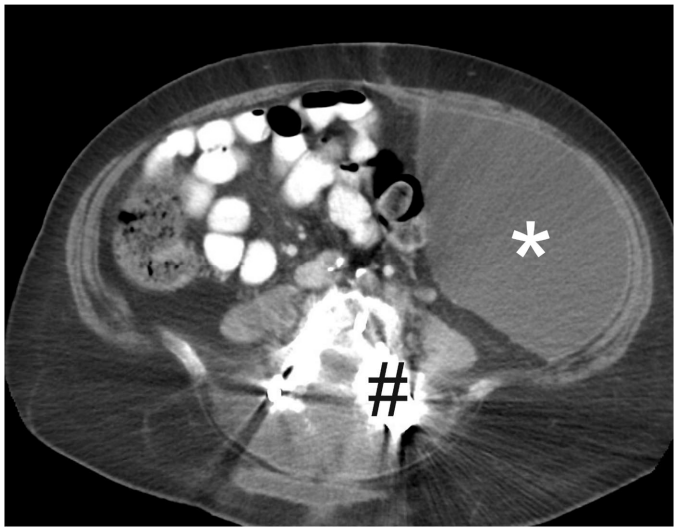
Figure 9. Thoracic duct embolization in a 50-year-old woman with plastic bronchitis of unknown etiology. (**a**) Clinical photograph of a lymphatic non-inflammatory cast produced by the patient. The branching pattern indicates it originated from the airways and took the shape of the hollow structures from where it was formed. The patient indicated that she could sense the obstruction on the right side. (**b**) Thoracic duct lymphangiography executed in a similar fashion as the patient in Figure 7. Black arrows indicate a large abnormal collateral vessel tracking to the right mainstem bronchus and upper lobe airways. The topmost arrow indicates a pooling of contrast consistent with a leak. The black bracket indicates otherwise normal thoracic duct anatomy. This thoracic duct was embolized in the same fashion as the patient in Figure 7.

9. Post-Operative Lymphocele

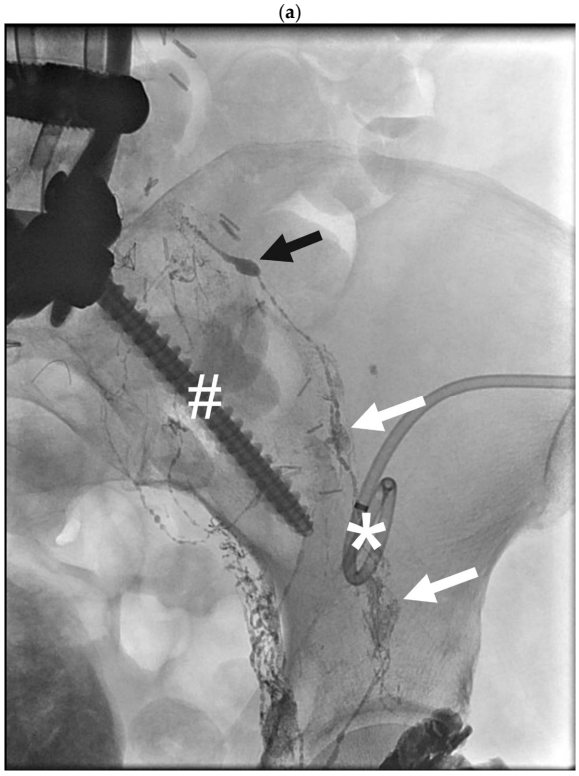
Post-operative lymphocele occurs after surgery when lymphatic fluid collects in the abdomen or pelvis without drainage and can result in anatomic compression of organs or vascular structures, causing abdominal pain or bulk symptoms. It may occur anytime lymphatic architecture is disrupted and can affect between 0.6 and 51% of patients [59,60]. Vascular compromise and ureteric obstruction after renal transplant are among the more concerning complications from lymphocele formation [59]. Lymph node dissections for colorectal and gynecological malignancies, renal transplantation, and radical prostatectomy are common causes of lymphocele formation; however, disruption of the retroperitoneal lymphatics has been observed after spinal surgery [61–64].

Initial diagnosis begins with fluid drainage and sampling, with fluid studies performed to rule out infection (fluid culture), creatinine (urine leak, urinoma), and hematoma. The presence of triglycerides in the fluid is not necessary for diagnosis, as disrupted lymphatics from the central circulation (and not from gut-draining mesenteric lymphatics) would not be carrying digested fats. Instead, high total protein and a lymphocyte count >70% are diagnostic indicators that a post-operative lymphocele has formed.

Treatment may involve embolization with a mixture of ethiodized oil and glue through direct intranodal puncture and injection [65–67], and/or sclerotherapy through existing drain access into the collection. Technical descriptions of lymphocele management are described in Figure 10. Techniques for sclerotherapy have been adopted from the treatment literature for lymphatic malformations and cysts and are well described and reported with povidone-iodine, doxycycline, and ethanol [68–70].



(**a**)

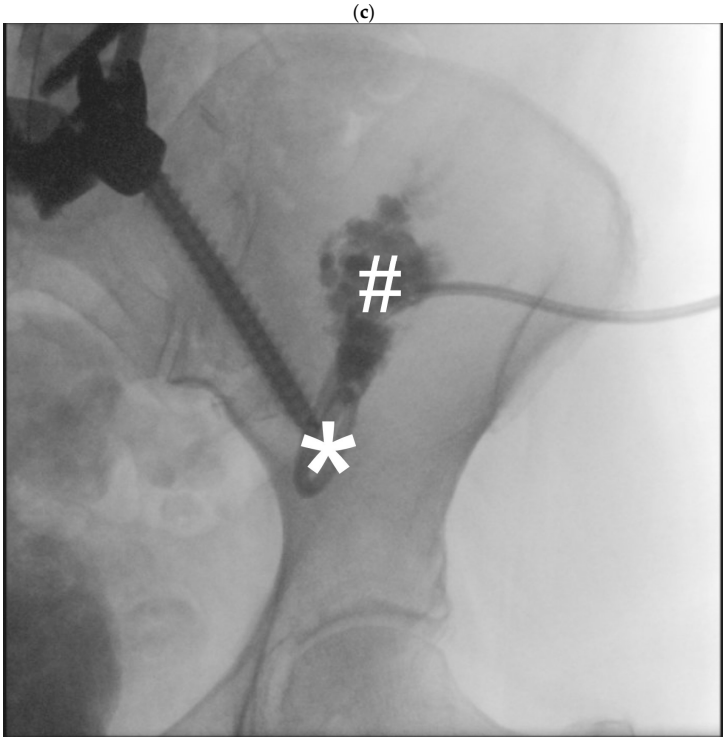


(**b**)

Figure 10. *Cont.*



(**c**)



(**d**)

Figure 10. Embolization and sclerotherapy of a post-operative lymphopseudoaneurysm and lymphocele, respectively, in a 62-year-old woman after posterior lumbar fusion. (**a**) A contrast-enhanced axial CT scan through the abdomen shows a large fluid collection in the left abdomen (*). Streak artifact from spinal hardware is shown (#). The fluid was found to be high in lymphocytes, but low in triglycerides suggestive of a non-chylous lymphocele. (**b**) A 25G needle access into an inguinal lymph node on the left side (not pictured) with ethiodized oil injection for fluoroscopic lymphangiography. The black arrow indicates the presence of a lymphopseudoaneurysm, or a contained lymphatic leak. The white arrows represent sentinel nodes downstream from the site of access. A drain (*) is pictured within the fluid collection. Spinal hardware is again seen (#). (**c**) Magnified view of a direct puncture of the lymphopseudoaneurysm (black arrow) with a long 22G needle (white arrow), seen en-face. This leak was embolized with 1:1 glue/ethiodized oil ratio. (**d**) Contrast is injected through the drain (*) and opacifies the fluid collection (#) to estimate the volume of sclerosant to treat the collection. This patient received 30 cc of doxycycline solution in sterile water at a concentration of 20 mg/mL.

Outcomes of embolization are favorably reported, with an 80% clinical success rate after 1–2 procedures, achieved within 7 days of embolization of the identified leak [65]. Sclerotherapy yields varied results and is directly related to the size of the lymphocele at the time of treatment [70]. Kim et al. report a 76.5% and 92.9% clinical success rate in non-infected and infected lymphoceles, respectively, with rare complications, including expected post-procedural pain and swelling. However, the need for multiple repeated sclerotherapies is often necessary [70,71].

10. Protein-Losing Enteropathy and Chylous Ascites

Disturbance of hepatic lymphatic flow can result from elevated central venous pressure, usually secondary to congenital heart disease and Fontan circulation, abnormal lymphogenesis due to somatic genetic alterations, absence of thoracic duct, or trauma [26,72]. Instead of following the normal drainage pathway into the cisterna chyli, hepatic lymph would be diverted to alternative lymphatic collaterals, most commonly into the duodenum and small bowel, resulting in protein-losing enteropathy and chylous ascites [73].

Excess protein loss into the intestinal tract characterizes protein-losing enteropathy (PLE). This condition can arise as a primary disorder (also known as primary intestinal lymphangiectasia) or, more frequently, as a secondary process related to increased lymphatic production, lymphatic obstruction, or enhanced mucosal permeability. PLE typically presents with symptoms such as severe diarrhea, swelling in the extremities, accumulation of fluid in the abdomen, difficulty tolerating food, and impaired wound healing. Given the non-specific nature of these symptoms, additional laboratory tests are necessary, including checks for low albumin, calcium, lymphocyte count, and immunoglobulin levels. The definitive diagnostic test involves measuring elevated stool alpha-1 antitrypsin levels over a 24 h period and comparing them to serum levels (alpha-1 antitrypsin clearance). PLE was initially observed in connection with congenital heart disease as a complication following total cavopulmonary anastomosis. Subsequent reports in this population have shown a prevalence of 5–12% and a high mortality rate, with 50% of patients succumbing within 5 years of diagnosis [74,75].

The most common abnormal imaging finding in patients with PLE is duodenal wall enhancement with leakage of contrast into the duodenal lumen [29,76] (Figure 11). This reflects the pathophysiology of abnormal flow patterns through the hepaticoduodenal lymphatic connection as a result of increased central venous pressure, absent thoracic duct, or abnormal lymphogenesis. This also corresponds to the endoscopic findings of "snowflake" appearance, representing dilated mucosal and submucosal lymphatic vessels, which are prone to rupture and leakage [77].

Other abnormal imaging features include chylous ascites, mesenteric lymphatic edema, retrograde mesenteric lymphatic flow, and retrograde flow into the peripancreatic lymphatic network. It is not uncommon to observe other associated abnormalities in the central conducting lymphatic system, including absence or dysplasia of the thoracic duct, abnormal lymphatic collateralization away from the midline, and chylous effusions [29,76].

Treatment for PLE also varies among institutions and generally includes diuresis, albumin, and electrolyte supplementation. These treatments mainly address the underlying symptoms but fail to address the cause of the disease. The addition of steroids, particularly enteral budesonide, has demonstrated significant improvement in both symptoms and laboratory values while decreasing mortality. However, not all patients respond, and over time, even responders will develop significant side effects from chronic steroid use [75].

In patients with PLE refractory to medical therapies, or with significant treatment side effects, there are percutaneous interventional options available. Percutaneous transhepatic lymphatic embolization (PTLE) has been shown to provide symptomatic improvement for

PLE patients secondary to congenital heart disease in short to mid-term follow-up [73,77]. In the 2017 series by Itkin et al., patients receiving n-butyl cyanoacrylate (n-BCA) glue embolization showed 50% sustained improvement in serum albumin levels with a mean follow-up of 149 days [77]. In another series in 2019 by Maleux et al., 6/7 patients showed normalization of serum albumin levels with a mean follow-up of 310 days [73].

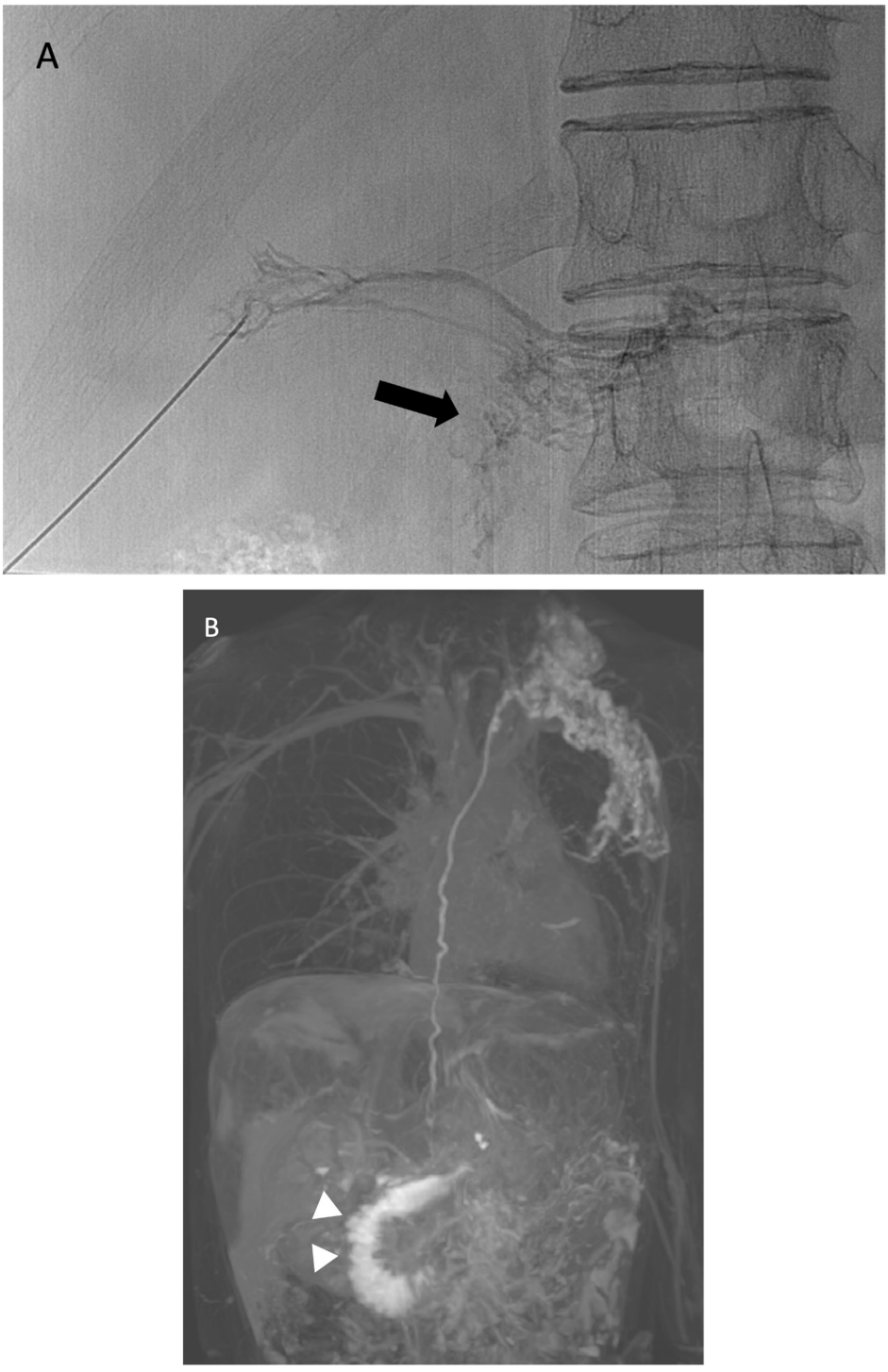


Figure 11. *Cont.*

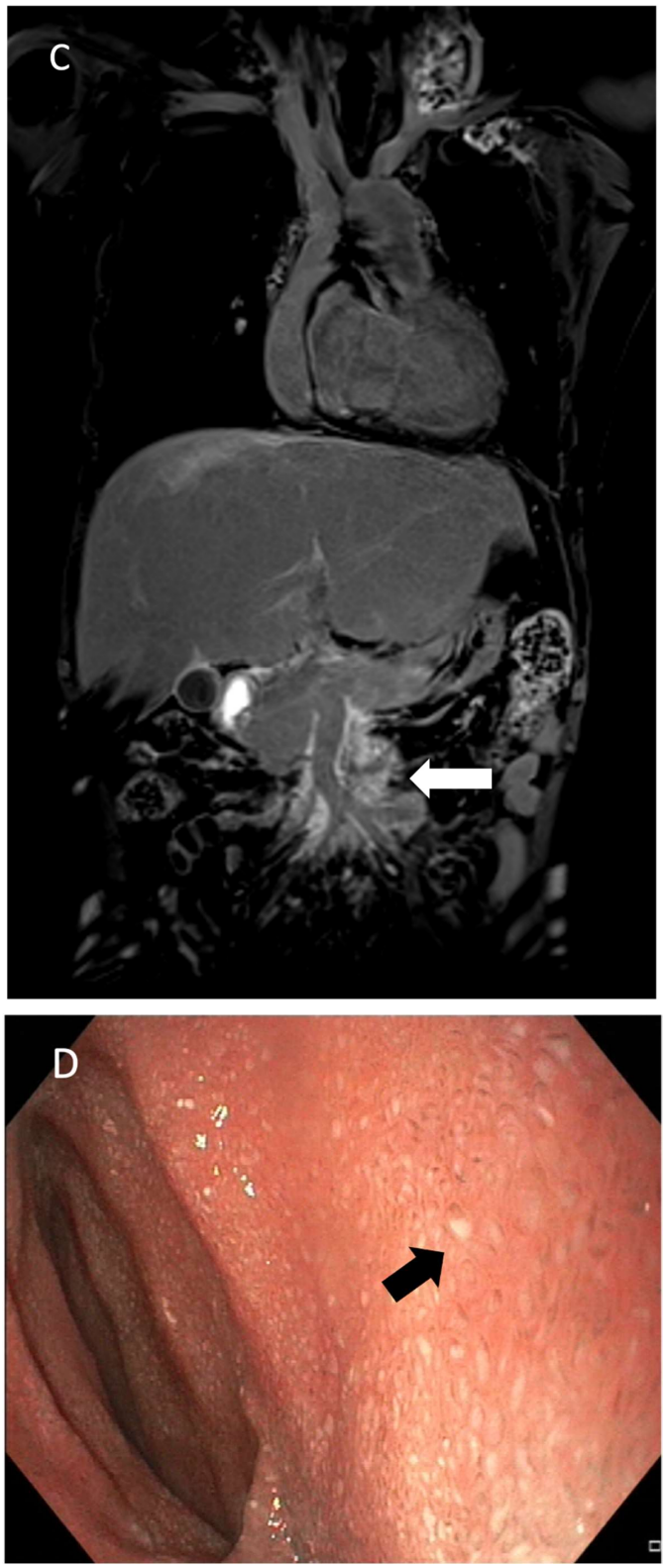


Figure 11. A 21-year-old girl with a history of hypoplastic left heart syndrome and Fontan's operation. (**A**) Conventional fluorosocpic intrahepatic lymphangiogram demonstrated abnormal hepatico-duodenal connections and dilated lymphatic channels (black arrow) along the duodenal wall. (**B**) Minimum-intensity-projection (MIP) coronal image of post-contrast T1-weighed intrahepatic DCMRL showed contrast leakage into duodenal lumen (white arrowheads). (**C**) Coronal image of post-contrast T1-weighed intrahepatic DCMRL showed abnormal enhancement of mesenteric lymphatics (white arrow), indicating retrograde mesenteric flow. (**D**) Endoscopic photo at second part of duodenum showed multiple tiny mucosal white specks (black arrow), compatible with snowflake appearance of lymphangectasia.

The technical procedure is similar to that of performing an intrahepatic lymphangiogram. Using ultrasound and fluoroscopic guidance, the intrahepatic lymphatics are accessed with 22G or 25G needles. Water-soluble contrast is injected to localize the leakage point or abnormal lymphatic network. In some institutions, additional injection of methylene blue is performed under concomitant upper endoscopy to visualize the abnormal perfusion/leaks, as well as to exclude any connections or contamination of the biliary system [78]. When these networks are identified, they are subsequently embolized with a 25% n-BCA glue/lipidol mixture (Figure 12). Visualization of the embolization often results in glue being seen entering the duodenal lumen through endoscopy and fluoroscopy, confirming occlusion of the abnormal fistulae.

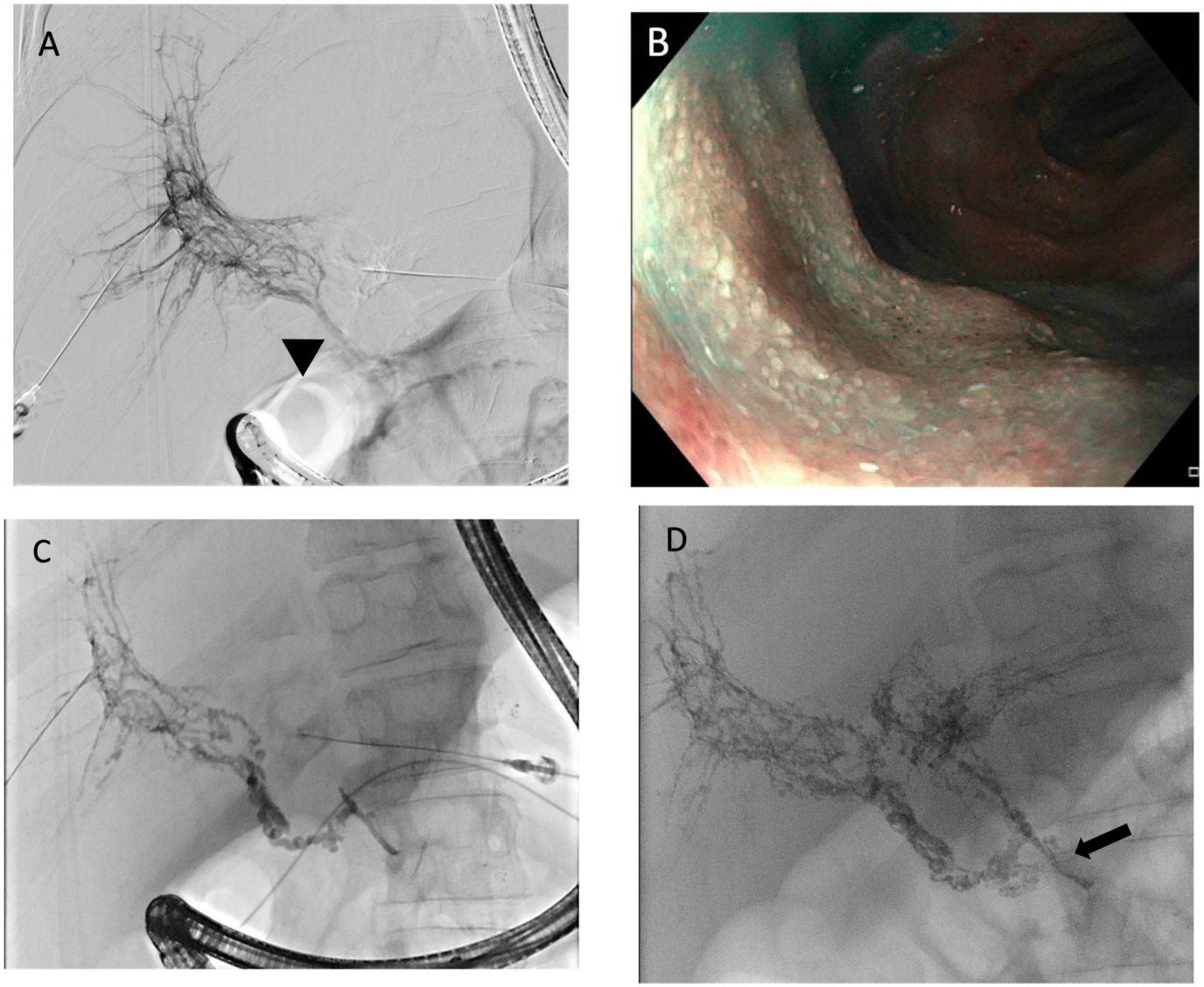


Figure 12. A 16-year-old girl with somatic KRAS mutation and protein-losing enteropathy. (**A**) A conventional fluoroscopic hepatic lymphangiogram showed an abnormal hepatico-duodenal connection (black arrowhead). (**B**) Endoscopic view confirmed leakage of hepatic lymph into duodenal lumen upon injection of methylene blue dye using the needle positioned at intrahepatic lymphatic channel. (**C**) Spot fluoroscopic image showed injection of 25% nBCA/lipiodol mixture using the needle located at right-sided intrahepatic lymphatic channels. (**D**) Spot fluoroscopic image after injection of glue mixture showed occlusion of hepatico-duodenal lymphatic connection (black arrow). However, the therapeutic effect is short-lived and the PLE recurred within 1 week.

Although generally safe, PTLE adverse events may include glue migration to adjacent vessels/ducts (venous, arterial, and biliary systems) and duodenal bleeding [73]. Care should be taken to avoid transgressing the portal vein during initial access of periportal hepatic lymphatic channels. Duodenal bleeding is likely due to the caustic effect of the embolic glue on the intestinal mucosa, which may be related to the type of glue used. Ethiodized oil was implicated in duodenal bleeding, whereas nBCA glue showed no such effect [77]. However, Maleux et al. reported a case of duodenal bleeding with nBCA. The exact mechanism remains unclear [73].

Although percutaneous transhepatic lymphatic embolization offers temporary relief for PLE, some patients experience treatment failure or recurrence, possibly due to the existence of abnormal extrahepatic lymphatic connections. To address these connections, new techniques have been developed, including percutaneous periduodenal embolization, retrograde endoscopic embolization of lymphatic leakage sites in the duodenum, and duodenal mucosal radiofrequency ablation [79–81]. These methods have shown varying degrees of clinical success, ranging from 50 to 70%. However, most studies have small sample sizes and limited follow-up periods. For patients with minimal or no response, or those experiencing recurring disease, several theories exist regarding potential factors, such as the condition of central lymphatics, progressive multicompartment disease, PLE duration, timing of PLE intervention post-diagnosis, and early consideration of transplantation. This underscores the necessity for further investigation in this field.

11. Conclusions

In summary, knowledge of lymphatic embryology, anatomy, physiology, and pathophysiology has led to profound advancements in medical imaging and intervention of disorders of lymphatic flow. Continued understanding of the genetic and anatomic origins of lymphatic disruption may provide new insights into the management of these disorders with advanced interventional and medical therapy.

Author Contributions: Conceptualization, F.J.B. and K.F.K.F.; methodology, F.J.B. and K.F.K.F.; writing—original draft preparation, F.J.B. and K.F.K.F.; writing—review and editing, F.J.B. and K.F.K.F.; supervision, F.J.B. and K.F.K.F. All authors have read and agreed to the published version of the manuscript.

Funding: This research received no external funding.

Institutional Review Board Statement: This review article requires no IRB approval for the purposes of literature review and educational examples.

Informed Consent Statement: Not Applicable for a review article.

Data Availability Statement: No original data gathered for this review article.

Conflicts of Interest: The authors declare no relevant conflicts of interest.

References

1. Goswami, A.K.; Khaja, M.S.; Downing, T.; Kokabi, N.; Saad, W.E.; Majdalany, B.S. Lymphatic Anatomy and Physiology. *Semin. Interv. Radiol.* **2020**, *37*, 227–236. [CrossRef]
2. Jeong, J.; Tanaka, M.; Iwakiri, Y. Hepatic lymphatic vascular system in health and disease. *J. Hepatol.* **2022**, *77*, 206–218. [CrossRef]
3. Tanaka, M.; Iwakiri, Y. The Hepatic Lymphatic Vascular System: Structure, Function, Markers, and Lymphangiogenesis. *Cell. Mol. Gastroenterol. Hepatol.* **2016**, *2*, 733–749. [CrossRef]
4. Witte, M.H.; Jones, K.; Wilting, J.; Dictor, M.; Selg, M.; McHale, N.; Gershenwald, J.E.; Jackson, D.G. Structure function relationships in the lymphatic system and implications for cancer biology. *Cancer Metastasis Rev.* **2006**, *25*, 159–184. [CrossRef]
5. van der Putte, S.C. The development of the lymphatic system in man. *Adv. Anat. Embryol. Cell Biol.* **1975**, *51*, 3–60.

6. Rockson, S.G. Embryology of the Lymphatic System and Lymphangiogenesis. In *Lymphedema: A Concise Compendium of Theory and Practice [Internet]*; Lee, B.B., Rockson, S.G., Bergan, J., Eds.; Springer International Publishing: Cham, Switzerland, 2018; pp. 47–55. [CrossRef]
7. Oliver, G. Lymphatic vasculature development. *Nat. Rev. Immunol.* **2004**, *4*, 35–45. [CrossRef]
8. Hogan, B.M.; Bos, F.L.; Bussmann, J.; Witte, M.; Chi, N.C.; Duckers, H.J.; Schulte-Merker, S. Ccbe1 is required for embryonic lymphangiogenesis and venous sprouting. *Nat. Genet.* **2009**, *41*, 396–398. [CrossRef]
9. Bos, F.L.; Caunt, M.; Peterson-Maduro, J.; Planas-Paz, L.; Kowalski, J.; Karpanen, T.; van Impel, A.; Tong, R.; Ernst, J.A.; Korving, J.; et al. CCBE1 is essential for mammalian lymphatic vascular development and enhances the lymphangiogenic effect of vascular endothelial growth factor-C in vivo. *Circ. Res.* **2011**, *109*, 486–491. [CrossRef]
10. Wigle, J.T.; Chowdhury, K.; Gruss, P.; Oliver, G. Prox1 function is crucial for mouse lens-fibre elongation. *Nat. Genet.* **1999**, *21*, 318–322. [CrossRef]
11. Yang, Y.; García-Verdugo, J.M.; Soriano-Navarro, M.; Srinivasan, R.S.; Scallan, J.P.; Singh, M.K.; Epstein, J.A.; Oliver, G. Lymphatic endothelial progenitors bud from the cardinal vein and intersomitic vessels in mammalian embryos. *Blood* **2012**, *120*, 2340–2348. [CrossRef]
12. Hägerling, R.; Pollmann, C.; Andreas, M.; Schmidt, C.; Nurmi, H.; Adams, R.H.; Alitalo, K.; Andresen, V.; Schulte-Merker, S.; Kiefer, F. A novel multistep mechanism for initial lymphangiogenesis in mouse embryos based on ultramicroscopy. *MBO J.* **2013**, *32*, 629–644. [CrossRef]
13. François, M.; Short, K.; Secker, G.A.; Combes, A.; Schwarz, Q.; Davidson, T.-L.; Smyth, I.; Hong, Y.-K.; Harvey, N.L.; Koopman, P. Segmental territories along the cardinal veins generate lymph sacs via a ballooning mechanism during embryonic lymphangiogenesis in mice. *Dev. Biol.* **2011**, *364*, 89–98. [CrossRef]
14. Wigle, J.T.; Harvey, N.; Detmar, M.; Lagutina, I.; Grosveld, G.; Gunn, M.D.; Jackson, D.G.; Oliver, G. An essential role for Prox1 in the induction of the lymphatic endothelial cell phenotype. *EMBO J.* **2002**, *21*, 1505–1513. [CrossRef]
15. Hu, Z.; Zhao, X.; Wu, Z.; Qu, B.; Yuan, M.; Xing, Y.; Song, Y.; Wang, Z. Lymphatic vessel: Origin, heterogeneity, biological functions and therapeutic targets. *Signal Transduct. Target. Ther.* **2024**, *9*, 1–37. [CrossRef]
16. Yaniv, K.; Isogai, S.; Castranova, D.; Dye, L.; Hitomi, J.; Weinstein, B.M. Live imaging of lymphatic development in the zebrafish. *Nat. Med.* **2006**, *12*, 711–716. [CrossRef]
17. Buttler, K.; Kreysing, A.; von Kaisenberg, C.S.; Schweigerer, L.; Gale, N.; Papoutsi, M.; Wilting, J. Mesenchymal cells with leukocyte and lymphendothelial characteristics in murine embryos. *Dev. Dyn.* **2006**, *235*, 1554–1562. [CrossRef]
18. Suami, H.; Kato, S. Anatomy of the Lymphatic System and Its Structural Disorders in Lymphoedema. In *Lymphedema: A Concise Compendium of Theory and Practice [Internet]*; Lee, B.B., Rockson, S.G., Bergan, J., Eds.; Springer International Publishing: Cham, Switzerland, 2018; pp. 57–78. [CrossRef]
19. Johnson, O.W.; Chick, J.F.B.; Chauhan, N.R.; Fairchild, A.H.; Fan, C.-M.; Stecker, M.S.; Killoran, T.P.; Suzuki-Han, A. The thoracic duct: Clinical importance, anatomic variation, imaging, and embolization. *Eur. Radiol.* **2015**, *26*, 2482–2493. [CrossRef]
20. Mazzei, F.G.; Gentili, F.; Guerrini, S.; Squitieri, N.C.; Guerrieri, D.; Gennaro, P.; Scialpi, M.; Volterrani, L.; Mazzei, M.A. MR Lymphangiography: A Practical Guide to Perform It and a Brief Review of the Literature from a Technical Point of View. *BioMed Res. Int.* **2017**, *2017*, 2598358. [CrossRef]
21. Calderwood, A.; Thompson, B.; Ho-Shon, K.; Suami, H. Overview of magnetic resonance lymphography for imaging lymphoedema. *Plast. Aesthetic Res.* **2021**, *8*, 1–14. [CrossRef]
22. Pieper, C.C. Nodal and Pedal MR Lymphangiography of the Central Lymphatic System: Techniques and Applications. *Semin. Interv. Radiol.* **2020**, *37*, 250–262. [CrossRef]
23. Lee, E.W.; Shin, J.H.; Ko, H.K.; Park, J.; Kim, S.H.; Sung, K.-B. Lymphangiography to Treat Postoperative Lymphatic Leakage: A Technical Review. *Korean J. Radiol.* **2014**, *15*, 724–732. [CrossRef] [PubMed]
24. Fung, K.F.K.; Chen, H.-S.R.; Ng, W.K.C.; Che, K.Y.J.; Poon, M.Y.; Lun, K.S.; Kan, Y.L.E. Feasibility of contrast-enhanced ultrasound in confirming intranodal needle position for dynamic contrast-enhanced magnetic resonance lymphangiography in children. *Pediatr. Radiol.* **2023**, *53*, 2137–2143. [CrossRef] [PubMed]
25. Wagenpfeil, J.; Kupczyk, P.A.; Henkel, A.; Geiger, S.; Köster, T.; Luetkens, J.A.; Schild, H.H.; Attenberger, U.I.; Pieper, C.C. Ultrasound-guided needle positioning for nodal dynamic contrast-enhanced MR lymphangiography. *Sci. Rep.* **2022**, *12*, 3621. [CrossRef] [PubMed]
26. Ramirez-Suarez, K.I.; Tierradentro-Garcia, L.O.; Stern, J.A.; Dori, Y.; Escobar, F.A.; Otero, H.J.; Rapp, J.B.; Smith, C.L.; Krishnamurthy, G.; Biko, D.M. State-of-the-art imaging for lymphatic evaluation in children. *Pediatr. Radiol.* **2022**, *53*, 1380–1390. [CrossRef]
27. Matsumoto, S.; Mori, H.; Tada, I. Successful Demonstration of Post-Operative Lymphatic Fistula by Percutaneous Transhepatic Lymphography: Case Reports. *Clin. Radiol.* **2000**, *55*, 485–486. [CrossRef]
28. Ramirez-Suarez, K.I.; Tierradentro-Garcia, L.O.; Smith, C.L.; Krishnamurthy, G.; Escobar, F.A.; Otero, H.J.; Rapp, J.B.; Dori, Y.; Biko, D.M. Dynamic contrast-enhanced magnetic resonance lymphangiography. *Pediatr. Radiol.* **2022**, *52*, 285–294. [CrossRef]

29. Biko, D.M.; Smith, C.L.; Otero, H.J.; Saul, D.; White, A.M.; DeWitt, A.; Glatz, A.C.; Piccoli, D.A.; Mamula, P.; Rome, J.J.; et al. Intrahepatic dynamic contrast MR lymphangiography: Initial experience with a new technique for the assessment of liver lymphatics. *Eur. Radiol.* **2019**, *29*, 5190–5196. [CrossRef]
30. Wong, D.; Fung, K.F.K.; Chen, H.-S.R.; Lun, K.S.; Kan, Y.L.E. Intranodal cone-beam computed tomographic lymphangiography with water-soluble iodinated contrast agent for evaluating chylothorax in infants—Preliminary experience at a single institution. *Pediatr. Radiol.* **2023**, *53*, 179–183. [CrossRef]
31. Kirschen, M.P.; Dori, Y.; Itkin, M.; Licht, D.J.; Ichord, R.; Vossough, A. Cerebral Lipiodol Embolism after Lymphatic Embolization for Plastic Bronchitis. *J. Pediatr.* **2016**, *176*, 200–203. [CrossRef]
32. Schwartz, F.R.; James, O.; Kuo, P.H.; Witte, M.H.; Koweek, L.M.; Pabon-Ramos, W.M. Lymphatic Imaging: Current Noninvasive and Invasive Techniques. *Semin. Interv. Radiol.* **2020**, *37*, 237–249. [CrossRef]
33. Bhatnagar, M.; Fisher, A.; Ramsaroop, S.; Carter, A.; Pippard, B. Chylothorax: Pathophysiology, diagnosis, and management—A comprehensive review. *J. Thorac. Dis.* **2024**, *16*, 1645–1661. [CrossRef] [PubMed]
34. Bialkowski, A.; Poets, C.F.; Franz, A.R.; Erhebungseinheit für Seltene Pädiatrische Erkrankungen in Deutschland Study Group. Congenital chylothorax: A prospective nationwide epidemiological study in Germany. *Arch. Dis. Child.-Fetal Neonatal Ed.* **2015**, *100*, F169–F172. [CrossRef] [PubMed]
35. Haines, C.; Walsh, B.; Fletcher, M.; Davis, P.J. Chylothorax development in infants and children in the UK. *Arch. Dis. Child.* **2014**, *99*, 724–730. [CrossRef]
36. Chen, S.; Zhao, Y.; Chen, H. Risk factors of chylothorax after esophagectomy. *J. Thorac. Dis.* **2019**, *11*, 1749–1752. [CrossRef]
37. Rudrappa, M.; Paul, M. Chylothorax. In *StatPearls [Internet]*; StatPearls Publishing: Treasure Island, FL, USA, 2023. Available online: http://www.ncbi.nlm.nih.gov/books/NBK459206/ (accessed on 21 December 2023).
38. Ur Rehman, K.; Sivakumar, P. Non-traumatic chylothorax: Diagnostic and therapeutic strategies. *Breathe* **2022**, *18*, 210163. [CrossRef]
39. Dixon, J.B. Mechanisms of chylomicron uptake into lacteals. *Ann. N. Y. Acad. Sci.* **2010**, *1207* (Suppl. 1), E52–E57. [CrossRef]
40. Hussain, M.M. Intestinal Lipid Absorption and Lipoprotein Formation. *Curr. Opin. Infect. Dis.* **2014**, *25*, 200–206. [CrossRef]
41. Huggins, J.T. Chylothorax and cholesterol pleural effusion. *Semin. Respir. Crit. Care Med.* **2010**, *31*, 743–750. [CrossRef]
42. Prajapati, S.; Ramasamy, S.; Vats, M.; Neogi, S.; Kantamaneni, K.; Tudu, S.K. Effect of Octreotide on Lymphorrhea in Patients After Modified Radical Mastectomy for Carcinoma Breast: A Randomized Controlled Trial. *Cureus* **2021**, *13*, e19225. [CrossRef]
43. Yin, R.; Zhang, R.; Wang, J.; Yuan, L.; Hu, L.; Jiang, S.; Chen, C.; Cao, Y. Effects of somatostatin/octreotide treatment in neonates with congenital chylothorax. *Medicine* **2017**, *96*, e7594. [CrossRef]
44. Ntiamoah, P.; Mukhopadhyay, S.; Ghosh, S.; Mehta, A.C. Recycling plastic: Diagnosis and management of plastic bronchitis among adults. *Eur. Respir. Rev.* **2021**, *30*, 210096. [CrossRef] [PubMed]
45. Quysner, A.; Surani, S.; Roberts, D. Plastic Bronchitis. *West. J. Emerg. Med.* **2011**, *12*, 118–119. [PubMed]
46. Nayar, S.; Parmar, R.; Kulkarni, S.; Cherian, K.M. Treatment of Plastic Bronchitis. *Ann. Thorac. Surg.* **2007**, *83*, 1884–1886. [CrossRef]
47. Muller, A.F.; Mithal, A. A case of plastic bronchitis. *J. R. Soc. Med.* **1988**, *81*, 360. [CrossRef]
48. Patel, N.; Patel, M.; Inja, R.; Krvavac, A.; Lechner, A.J. Plastic Bronchitis in Adult and Pediatric Patients: A Review of its Presentation, Diagnosis, and Treatment. *Mo. Med.* **2021**, *118*, 363–373.
49. Dori, Y.; Keller, M.S.; Rome, J.J.; Gillespie, M.J.; Glatz, A.C.; Dodds, K.; Goldberg, D.J.; Goldfarb, S.; Rychik, J.; Itkin, M. Percutaneous Lymphatic Embolization of Abnormal Pulmonary Lymphatic Flow as Treatment of Plastic Bronchitis in Patients With Congenital Heart Disease. *Circulation* **2016**, *133*, 1160–1170. [CrossRef]
50. Chen, E.; Itkin, M. Thoracic Duct Embolization for Chylous Leaks. *Semin. Interv. Radiol.* **2011**, *28*, 63–74. [CrossRef]
51. Nadolski, G.J.; Itkin, M. Lymphangiography and thoracic duct embolization following unsuccessful thoracic duct ligation: Imaging findings and outcomes. *J. Thorac. Cardiovasc. Surg.* **2018**, *156*, 838–843. [CrossRef]
52. Cope, C.; Salem, R.; Kaiser, L.R. Management of chylothorax by percutaneous catheterization and embolization of the thoracic duct: Prospective trial. *J. Vasc. Interv. Radiol.* **1999**, *10*, 1248–1254. [CrossRef]
53. Cope, C.; Kaiser, L.R. Management of unremitting chylothorax by percutaneous embolization and blockage of retroperitoneal lymphatic vessels in 42 patients. *J. Vasc. Interv. Radiol.* **2002**, *13*, 1139–1148. [CrossRef]
54. Itkin, M.; Kucharczuk, J.C.; Kwak, A.; Trerotola, S.O.; Kaiser, L.R. Nonoperative thoracic duct embolization for traumatic thoracic duct leak: Experience in 109 patients. *J. Thorac. Cardiovasc. Surg.* **2010**, *139*, 584–590. [CrossRef] [PubMed]
55. Kim, P.H.; Tsauo, J.; Shin, J.H. Lymphatic Interventions for Chylothorax: A Systematic Review and Meta-Analysis. *J. Vasc. Interv. Radiol.* **2018**, *29*, 194–202.e4. [CrossRef] [PubMed]
56. Majdalany, B.S.; Saad, W.A.; Chick, J.F.B.; Khaja, M.S.; Cooper, K.J.; Srinivasa, R.N. Pediatric lymphangiography, thoracic duct embolization and thoracic duct disruption: A single-institution experience in 11 children with chylothorax. *Pediatr. Radiol.* **2017**, *48*, 235–240. [CrossRef] [PubMed]

57. Savla, J.J.; Itkin, M.; Rossano, J.W.; Dori, Y. Post-Operative Chylothorax in Patients with Congenital Heart Disease. *J. Am. Coll. Cardiol.* **2017**, *69*, 2410–2422. [CrossRef]
58. Laslett, D.; Trerotola, S.O.; Itkin, M. Delayed complications following technically successful thoracic duct embolization. *J. Vasc. Interv. Radiol. JVIR* **2012**, *23*, 76–79. [CrossRef]
59. Nerli, R.B.; Sushant, D.; Ghagane, S.C.; Nutalpati, S.; Mohan, S.; Dixit, N.S.; Neelagund, S.; Hiremath, M.B. Lymphocele Complications Following Renal Transplantation. *Indian J. Transplant.* **2019**, *13*, 273–276. [CrossRef]
60. Garcia-Tsao, G.; Sanyal, A.J.; Grace, N.D.; Carey, W. Prevention and management of gastroesophageal varices and variceal hemorrhage in cirrhosis. *Hepatology* **2007**, *46*, 922–938. [CrossRef]
61. Scheer, J.K.; Haddad, A.F.; Chan, A.K.; Eichler, C.M.; Tay, B.; Burch, S.; Chou, D.; Ames, C.P.; Mummaneni, P.V. Lymphocele after anterior lumbar interbody fusion: A review of 1322 patients. *J. Neurosurg. Spine* **2021**, *35*, 722–728. [CrossRef]
62. Guacheta-Bomba, P.L.; Guerrero, M.F.S.; Ramirez, G.; Garcia-Perdomo, H.A. Lymphocele Complication After Kidney Transplant: Current Literature Review and Management Algorithm. *Exp. Clin. Transplant.* **2023**, *21*, 855–859.
63. Tsaur, I.; Thomas, C. Risk factors, complications and management of lymphocele formation after radical prostatectomy: A mini-review. *Int. J. Urol.* **2019**, *26*, 711–716. [CrossRef]
64. Kim, H.Y.; Kim, J.W.; Kim, S.H.; Kim, Y.T.; Kim, J.H. An Analysis of the Risk Factors and Management of Lymphocele after Pelvic Lymphadenectomy in Patients with Gynecologic Malignancies. *Cancer Res. Treat.* **2004**, *36*, 377–383. [CrossRef] [PubMed]
65. Smolock, A.R.; Nadolski, G.; Itkin, M. Intranodal Glue Embolization for the Management of Postsurgical Groin Lymphocele and Lymphorrhea. *J. Vasc. Interv. Radiol.* **2018**, *29*, 1462–1465. [CrossRef] [PubMed]
66. Kwon, L.M.; Hur, S.; Jeong, C.W.; Jae, H.J.; Chung, J.W. Glue Embolization of Lymphopseudoaneurysm for Chylous Ascites after Retroperitoneal Surgery. *Korean J. Radiol.* **2021**, *22*, 376–383. [CrossRef] [PubMed]
67. Baek, Y.; Won, J.H.; Chang, S.-J.; Ryu, H.-S.; Song, S.-Y.; Yim, B.; Kim, J. Lymphatic Embolization for the Treatment of Pelvic Lymphoceles: Preliminary Experience in Five Patients. *J. Vasc. Interv. Radiol.* **2016**, *27*, 1170–1176. [CrossRef]
68. Bertino, F.J.; Hawkins, C.M. Contemporary management of extracranial vascular malformations. *Pediatr. Radiol.* **2023**, *53*, 1600–1617. [CrossRef]
69. Hawkins, C.M.; Chewning, R.H. Diagnosis and Management of Extracranial Vascular Malformations in Children: Arteriovenous Malformations, Venous Malformations, and Lymphatic Malformations. Semin Roentgenol [Internet]. 2019. Available online: http://www.sciencedirect.com/science/article/pii/S0037198X19300410 (accessed on 28 July 2019).
70. Mahrer, A.; Ramchandani, P.; Trerotola, S.O.; Shlansky-Goldberg, R.D.; Itkin, M. Sclerotherapy in the management of postoperative lymphocele. *J. Vasc. Interv. Radiol.* **2010**, *21*, 1050–1053. [CrossRef]
71. Kim, Y.; Jeon, G.S.; Choi, S.Y.; Kim, M.D.; Lee, S.J. Evaluation of sclerotherapy for the treatment of infected postoperative lymphocele. *Taiwan J. Obstet. Gynecol.* **2017**, *56*, 477–481. [CrossRef]
72. Pieper, C.C.; Wagenpfeil, J.; Henkel, A.; Geiger, S.; Köster, T.; Hoss, K.; Luetkens, J.A.; Hart, C.; Attenberger, U.I.; Müller, A. MR lymphangiography of lymphatic abnormalities in children and adults with Noonan syndrome. *Sci. Rep.* **2022**, *12*, 11164. [CrossRef]
73. Maleux, G.; Storme, E.; Cools, B.; Heying, R.; Boshoff, D.; Louw, J.J.; Frerich, S.; Malekzadeh-Milanii, S.; Hubrechts, J.; Brown, S.C.; et al. Percutaneous embolization of lymphatic fistulae as treatment for protein-losing enteropathy and plastic bronchitis in patients with failing Fontan circulation. *Catheter. Cardiovasc. Interv.* **2019**, *94*, 996–1002. [CrossRef]
74. Mertens, L.; Hagler, D.J.; Sauer, U.; Somerville, J.; Gewillig, M. Protein-losing enteropathy after the Fontan operation: An international multicenter study. *J. Thorac. Cardiovasc. Surg.* **1998**, *115*, 1063–1073. [CrossRef]
75. Alsaied, T.; Lubert, A.M.; Goldberg, D.J.; Schumacher, K.; Rathod, R.; Katz, D.A.; Opotowsky, A.R.; Jenkins, M.; Smith, C.; Rychik, J.; et al. Protein losing enteropathy after the Fontan operation. *Int. J. Cardiol. Congenit. Hear. Dis.* **2022**, *7*, 100338. [CrossRef] [PubMed]
76. Lemley, B.A.; Biko, D.M.; Dewitt, A.G.; Glatz, A.C.; Goldberg, D.J.; Saravanan, M.; O'byrne, M.L.; Pinto, E.; Ravishankar, C.; Rome, J.J.; et al. Intrahepatic Dynamic Contrast-Enhanced Magnetic Resonance Lymphangiography: Potential Imaging Signature for Protein-Losing Enteropathy in Congenital Heart Disease. *J. Am. Heart Assoc.* **2021**, *10*, e021542. [CrossRef] [PubMed]
77. Itkin, M.; Piccoli, D.A.; Nadolski, G.; Rychik, J.; DeWitt, A.; Pinto, E.; Rome, J.; Dori, Y. Protein-Losing Enteropathy in Patients with Congenital Heart Disease. *J. Am. Coll. Cardiol.* **2017**, *69*, 2929–2937. [CrossRef] [PubMed]
78. Smith, C.L.; Krishnamurthy, G.; Srinivasan, A.; Dori, Y. Lymphatic interventions in congenital heart disease. *Semin. Pediatr. Surg.* **2024**, *33*, 151419. [CrossRef]
79. Gartenberg, A.J.; Krishnamurthy, G.; Srinivasan, A.; Escobar, F.A.; Brownell, J.N.; Mamula, P.; O'byrne, M.L.; Dori, Y.; Smith, C.L. Intrahepatic and Periduodenal Embolization for Protein-Losing Enteropathy Patients with Congenital Heart Disease. *J. Am. Coll. Cardiol.* **2023**, *81*, 2476–2478. [CrossRef]

80. Itkin, M.; Teeple, E.A.; Spurrier, E.L.; Srivastava, S.; Rabinowitz, D.A. Transendoscopic retrograde hepatoduodenal lymphatic embolization as a treatment for protein losing enteropathy in patients with congenital heart disease. *J. Am. Coll. Cardiol.* **2022**, *79* (Suppl. 9), 1384. [CrossRef]
81. Husnain, A.; Aadam, A.A.; Reiland, A.; Salem, R.; Baker, J.; Nemcek, A.A.; Green, J.; Ganger, D.; De Freitas, R.A.; Riaz, A. Combined Percutaneous Transhepatic Lymphatic Embolization and Peroral Duodenal Mucosal Radiofrequency Ablation to Manage Protein-Losing Enteropathy. *J. Vasc. Interv. Radiol.* **2024**, *35*, 1351–1356.e1. [CrossRef]

Disclaimer/Publisher's Note: The statements, opinions and data contained in all publications are solely those of the individual author(s) and contributor(s) and not of MDPI and/or the editor(s). MDPI and/or the editor(s) disclaim responsibility for any injury to people or property resulting from any ideas, methods, instructions or products referred to in the content.